

A Geostatistical and Flow Simulation Study on a Real Training Image

Weishan Ren (wren@ualberta.ca)

Department of Civil & Environmental Engineering, University of Alberta

Abstract

A 12 cm by 18 cm slab of Eolian sandstone was scanned and formatted as a 600 by 900 pixel training image. A geostatistical study was performed using the training image: variograms were calculated with the Gaussian transform and the indicator transforms at the 9 deciles. The training image was used to provide a plausible model of heterogeneity for flow simulation. The color scale level was associated to permeability. Multiple realizations were created with sequential Gaussian and sequential indicator simulation. Then, the reference image and the simulated realizations were used in water flooding flow simulation. The geostatistical and flow simulation procedures are documented. The flow simulation results indicate that the geostatistical simulations tend to behave more homogeneously than the reference image. The large-scale non-linear connectivity of this reference image, and most geological formations for that matter, are important in flow modeling. The sequential Gaussian simulation gives a closer match than the sequential indicator simulation; the lack of correlation between indicator thresholds leads to a patchy pattern of heterogeneity with adjacent high and low values. This patchiness leads to a more homogeneous behavior than the Gaussian realizations.

This paper is the result of a warm-up study conducted by the author in the first two months of joining the Centre for Computational Geostatistics. The results motivate advanced geostatistical methods for characterizing heterogeneity and quantifying uncertainty.

Introduction

Flow simulation is an important tool to predict the production characteristics of a reservoir. Flow predictions require accurate (1) implementation of the flow physics in a numerical simulator, (2) specification of the fluid properties, and (3) heterogeneous porosity and permeability input arrays. The focus here is on the last consideration. In many cases, it is difficult to obtain an accurate assessment of heterogeneity because of sparse data and the unknown reservoir characteristics. Geostatistical simulation, especially the sequential Gaussian simulation (SGSIM) and the sequential indicator simulation (SISIM), have become widely accepted as premium methods to provide reliable estimation for porosity and permeability.

Porosity and permeability are not simply modeled by these techniques. The structural framework of the reservoir must be established. The stratigraphic framework and appropriate correlation surfaces must be established. The lithofacies are often modeled with other techniques that permit better characterization of non-linear connectivity, that is, object- or surface-based modeling. These important pre-processing steps are not considered here; however, their importance should be kept in mind.

A reference realization of heterogeneity is used to check the reliability of the estimation of geostatistical simulations and to assess the uncertainty associated with the estimation. This is one reference image that is much smaller than reservoir scale. Nevertheless, the complex non-linear

structure is similar to larger scale structures and we can gain a qualitative appreciation for how well the conventional geostatistical simulation algorithms perform.

In this study, the color of the training image was transformed into permeability values. These color changes are closely linked to the underlying porosity and permeability of the rock sample. Water flooding was simulated by Schlumberger's Eclipse software using the permeability data. The results are different significantly from a homogeneous distribution of porosity and permeability. The permeability generated from the training image is considered as the true or reference distribution of permeability.

Gaussian and indicator simulation (SGSIM and SISIM) (Deutsch, 1998a) are used to generate realizations of permeability. The histogram of permeability and all of the required variograms (Gaussian and indicator) are directly derived from the reference image. Of course, in practice, we would not have access to these reference statistics; however, the purpose of this study is not to highlight the problems of statistical inference. Rather, our goal is to understand how well geostatistical realizations of heterogeneity perform relative to a complex reference distribution. Ten realizations of permeability were created by each simulation method.

An important consideration in the study of heterogeneity is the size of the domain relative to the scale of heterogeneity. If the heterogeneities are small relative to the domain size, then the variability averages out and the domain will perform in a homogeneous manner. Some people refer to such a case as *heterogeneously homogeneous*. At the other extreme, when the heterogeneities are large relative to the domain size, they can appear deterministic and also perform in a homogeneous manner. A smaller image was extracted from the reference image to judge the results with a different domain size relative to the underlying heterogeneity.

An important objective of this report is to document the effect of heterogeneity and to demonstrate common geostatistical and flow simulation procedures. The training image will be provided to all CCG members for their own experimentation; it is always useful to have reference images for experimentation and development of new algorithms.

Training Image and Data File

The training image from the Eolian sandstone (Figure 1) has interesting geological features. A cyclicity of geological shapes is clearly shown in the vertical direction. There is a trend within several layers in the horizontal direction. The heterogeneities on this rock are not completely deterministic. We can reasonably consider them to be scale invariant over a large range of scales.

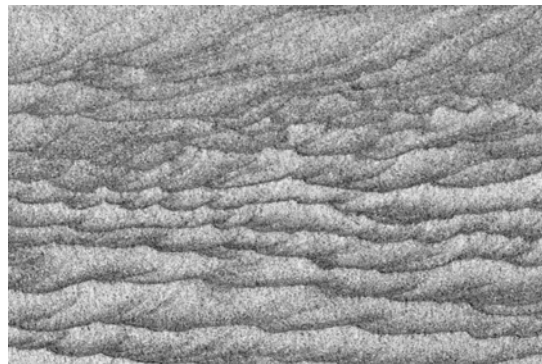


Figure 1: The training image scanned for this study.

The training image was transformed into a GSLIB format data file by the AM Lab's freeware, 3D Raster Viewer. In the transformation, the gray scales were decoded into numbers between 0 and 256. Figure 2 is the reproduced training image plotted from the generated data set: 0 is the pure white color and 256 is the pure black color. The reproduced image is almost identical to the original training image in Figure 1. The only difference is that the white color in the original image becomes the black in the reproduced image. The geological shapes and patterns are preserved during the transformation. This data is referred to as the TI data and will be considered the true reference data for testing.

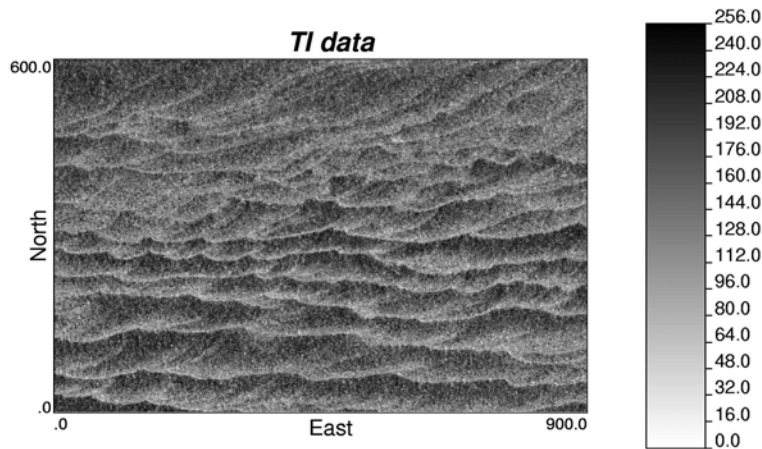


Figure 2: The image plot from the TI data converted to GSLIB format.

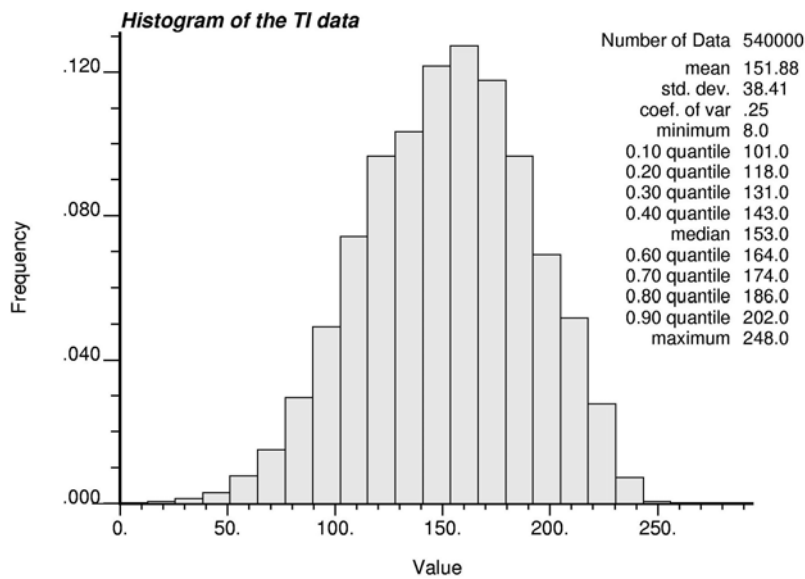


Figure 3: Histogram of the TI data.

The TI data is an exhaustive data set 900 cells are in X direction and 600 cells in the Y direction. There are 540,000 data. The data values vary from 8 to 248. The mean value is 151.88, and the standard deviation is 38.41. The histogram of the TI data (Figure 3) indicates that most of data are between 100 and 200.

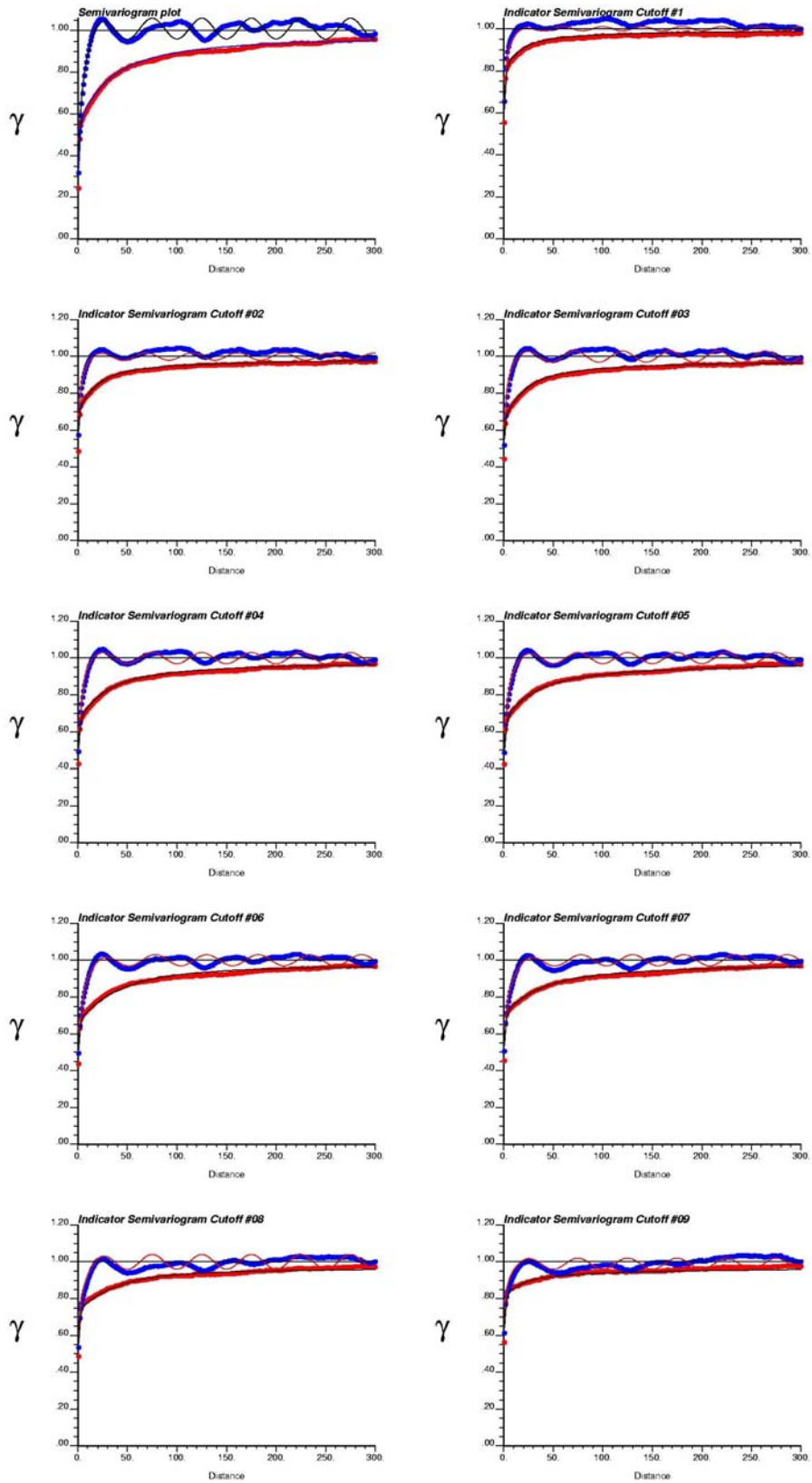


Figure 4: Normal scores variogram (upper left) and nine indicator variograms. Note the difference in the directional variograms and the cyclicity fitted to the experimental points.

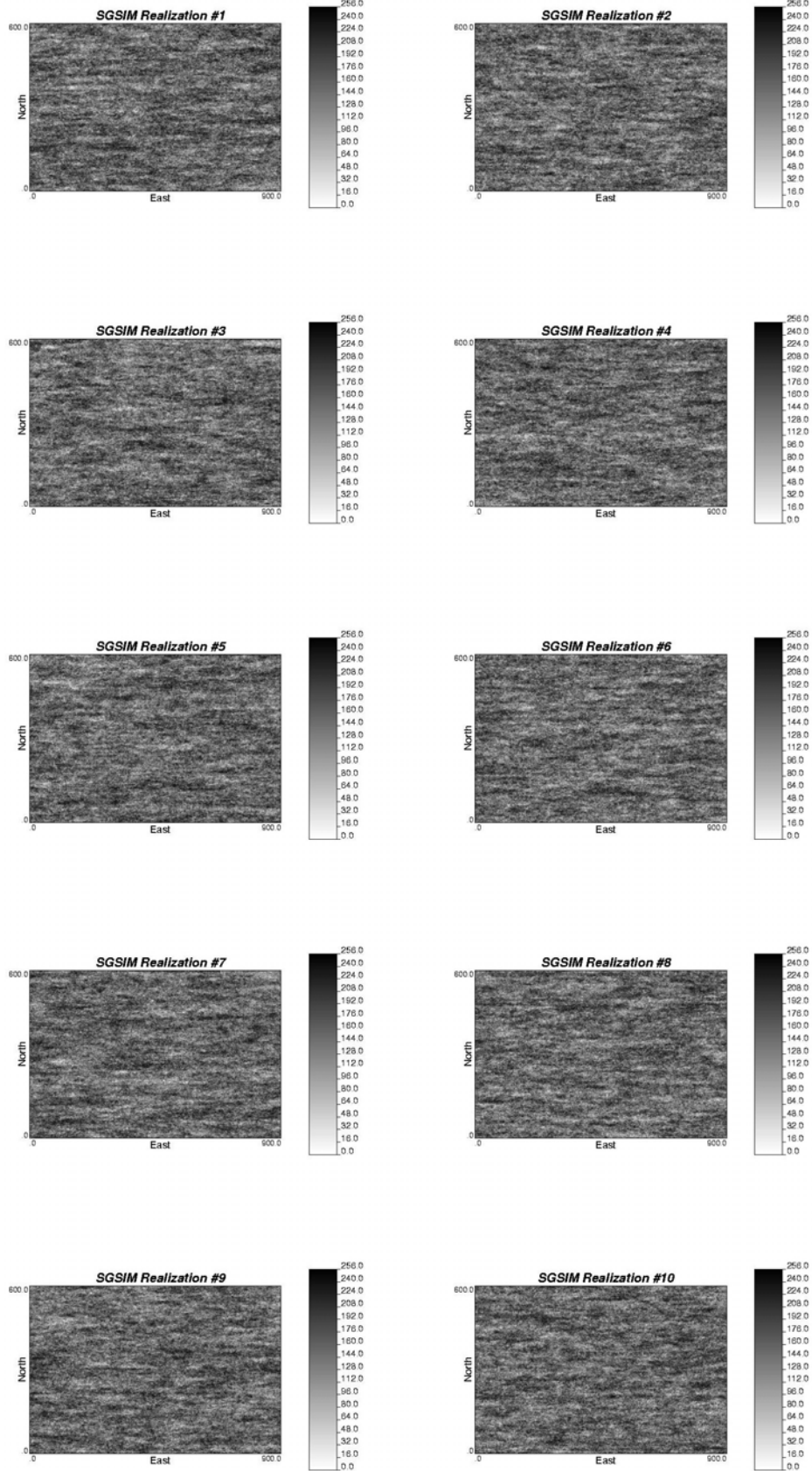


Figure 5: Ten SGSIM realizations of the TI data.

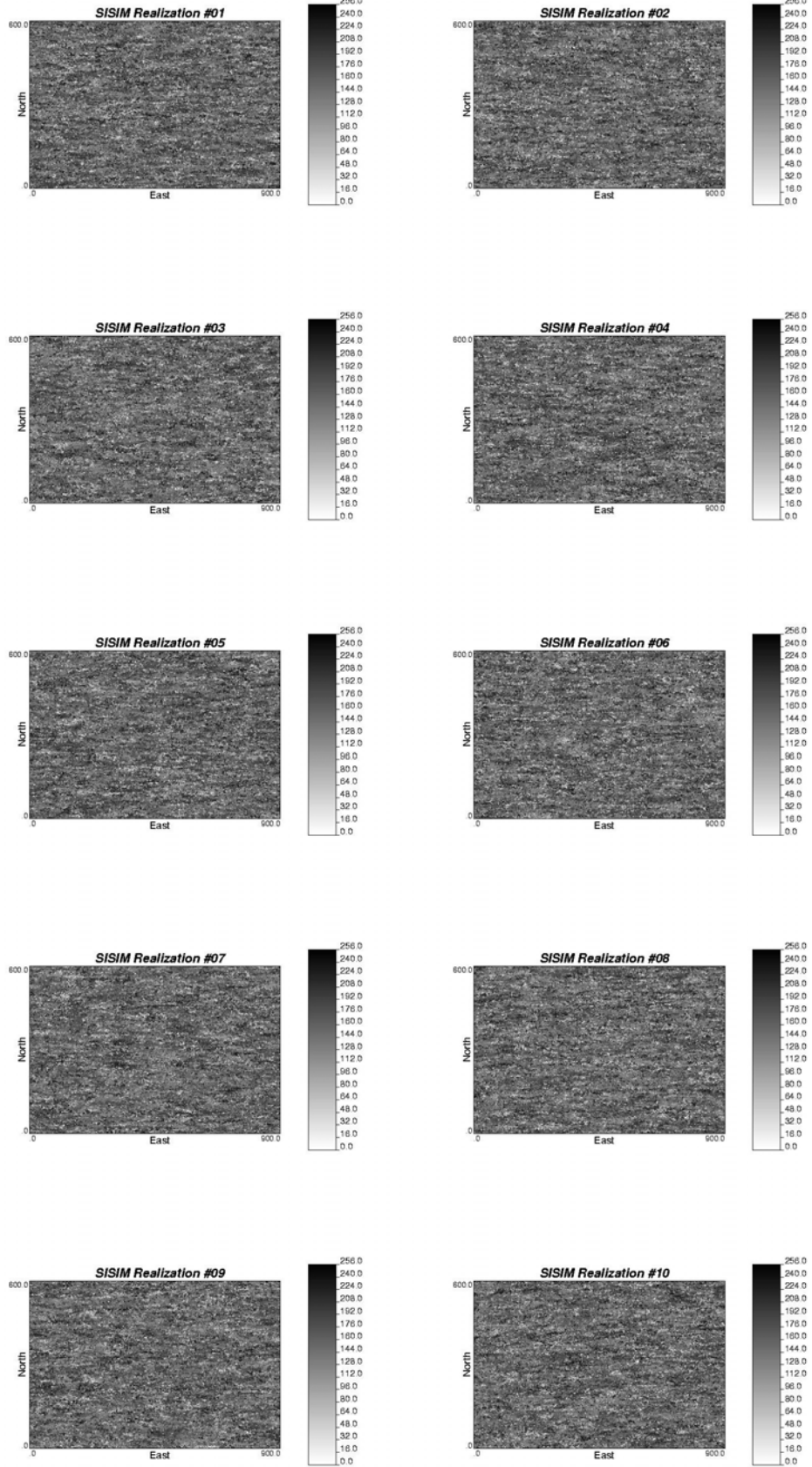


Figure 6: Ten SISIM realizations of the TI data.

Geostatistical Simulations

SGSIM and SISIM were used to generate 10 realizations. The histogram and variogram from the TI data were used as reference inputs. There was no local data for the sequential simulation.

The horizontal and vertical directions were chosen to calculate the semivariogram values based on the visual appearance of the training image. The 9 deciles were used to calculate the indicator variograms (Figure 3). The GAM program was used because the data are regularly spaced. The variograms and their models are shown in Figure 4. The top left variogram plot is the semivariogram of the Gaussian transform of the TI data. The rest of variogram plots correspond to the nine indicator semivariograms. The vertical variogram line shows cyclicity; a hole effect model was used in the variogram modeling to account for this cyclicity.

Ten SGSIM realizations are shown in Figure 5. Ten SISIM realizations are shown in Figure 6. Compare to the training image (Figure 2), the geological shapes are not well reproduced. The cyclicity in the vertical direction is apparent. The SGSIM realizations are similar to the SISIM realizations, except that color changes in the results of the SGSIM are smoother than that of SISIM. The patchiness of the SISIM realizations are characteristic.

Permeability Data

In general, permeability within a homogeneous lithofacies can be approximated by a lognormal distribution. The first step in converting the gray scale levels to permeability is the conversion of the values to a lognormal distribution. The lognormal transformation involves three steps. The first transform is the normal score transformation. The second transform is from the standard normal distribution to a non-standard normal distribution. Then, the last transform is from the non-standard normal distribution to a lognormal distribution. During the second transformation, the mean (α) and the standard deviation (β^2) of the non-standard normal distribution are calculated by the following two equations:

$$\alpha = \log(m) - \beta^2/2$$
$$\beta^2 = \log(1 + \sigma^2/m^2)$$

where m is the mean and σ^2 is the standard deviation of the target lognormal distribution (Deutsch, 1998b).

The TI data were transformed to a lognormal distribution with a mean of 100 mD and a standard deviation of 100 mD. The histogram of the lognormal TI data is shown in Figure 7. It shows a typical lognormal shape. The values vary from 1.33 mD to 3750 mD and most data are between 20 mD and 100 mD. Although this distribution appears quite variable, the permeability values behave very uniformly. Initial flow simulations led to results that are essentially the same as a homogeneous distribution (Figure 8). The water flow curves of the homogenous and heterogenous reservoir models are the same shape and very close to each other. There is a need to introduce high permeability conduits or low permeability barriers for the heterogeneity to have a significant effect.

The low and high permeability values were enhanced to increase the effect of heterogeneity. All values less than the 0.3-quantile were assigned a small value of 7.5 mD. All values larger than the 0.8-quantile were assigned a large value of 5000 mD. Then, the rest data were transformed into the lognormal distribution with a mean of 100 mD and a standard deviation of 100 mD. Figure 9 shows the resulting permeability values. The geological shapes and features have not changed. The new water production curve is plotted in Figure 8. A big difference is clearly

shown between the flow curves of the new heterogenous and homogenous models. Then, the same modified lognormal transform was applied to all SGSIM and SISIM realizations.

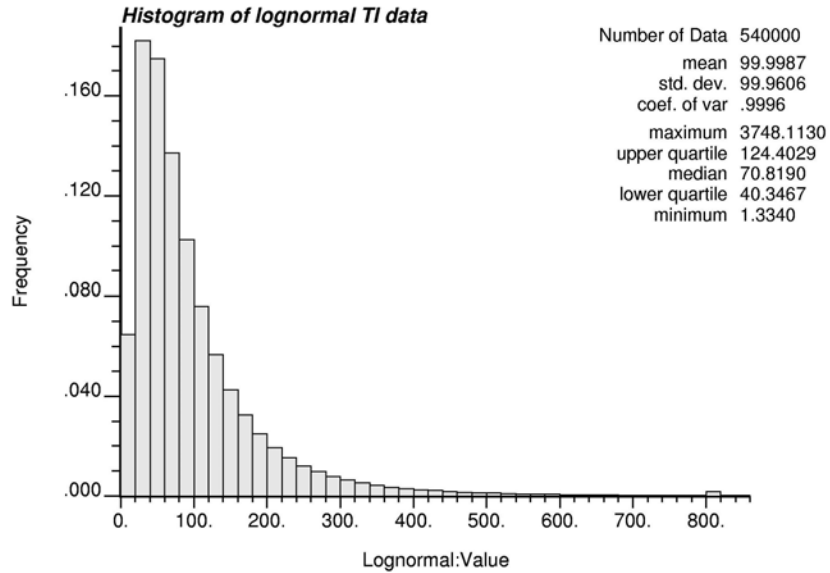


Figure 7: Histogram of lognormal TI data.

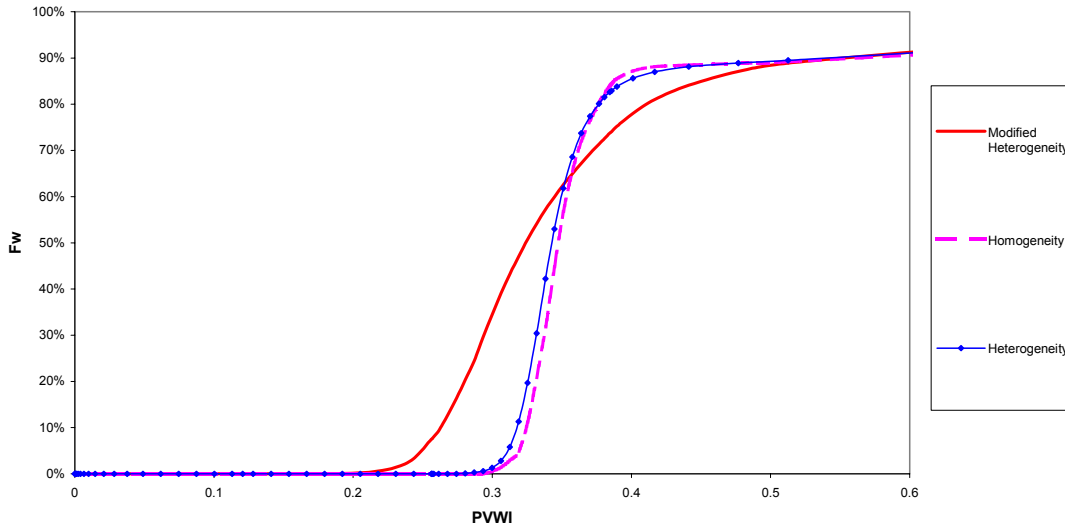


Figure 8: Flow curves of the heterogenous and homogenous models.

Using 540,000 data as permeability in a flow simulation requires 540,000 grid blocks for the reservoir model. Running flow simulation with such a large number of blocks takes a very long time and requires nearly 2GB RAM on a PC. This is not practical for the current situation where we want to run many different cases and realizations. In order to save time and run the simulation on an reasonably powerful PC, all data sets were scaled up to a coarser grid, that is, 225 by 150 with a total of 33750 grid blocks. The flow-based upscaling program FLOWSIM was used for the scale up. Figure 10 shows the data after scale up. The color changes in the image are more abrupt, but the geological shapes and features are still the same. After the scale up, all the data sets were changed to the Eclipse data format to be used as permeability.

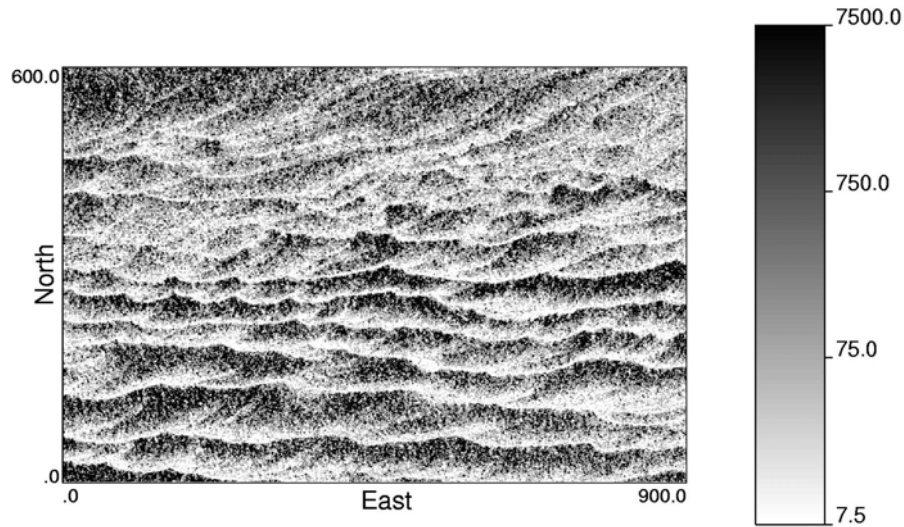


Figure 9: The training image after modified lognormal transform.

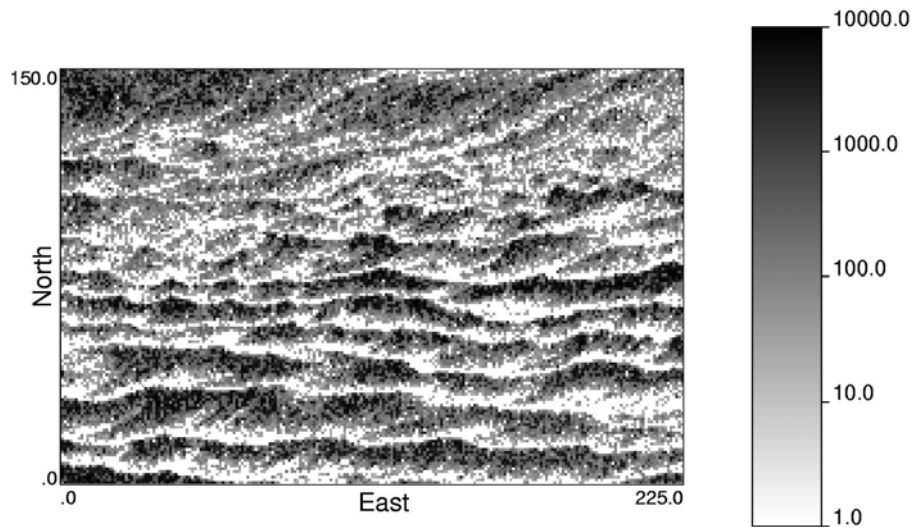


Figure 10: The training image after scale up.

Flow Simulations

The 2002A Eclipse black oil simulator was used for the flow simulation. The reservoir model was 1800 ft long, 1200 ft wide and 20 ft deep. As mentioned above, the 225 x 150 x 1 grid system was used. The porosity was set to be constant at 30%; the results are likely similar if porosity is correlated to permeability. Pressure was 4500 psi at the top of the reservoir (8450 ft depth). A horizontal injection well was drilled through the left hand side column of blocks, and a horizontal production well was also drilled through the right hand side column of blocks. The two wells were controlled by the reservoir volume rate of 3000 ft³/day. Injection and production start from the beginning and the simulation of water flooding was stopped after 1600 days.

A flow simulation with a homogeneous reservoir model was also performed. The homogenous reservoir model was exactly the same as the heterogenous models, except the permeability was set to the average value of the 100mD.

Three summary keywords are required to obtain the water flow performance curve. WWCT is the water cut, WVIT is the reservoir volume water injection total and FRPV is the reservoir pore volume. The water flow curve is the water fraction flow versus the pore volume of water injected. The water fraction flow (Fw) was using the WWCT data and the pore volume of water injected (PVWI) was calculated by dividing WVIT by FRPV. This curve is dimensionless and reflects physical features of a formation and properties of the fluids, and filter the effect of the well control, pressures, and specific rates.

The water flow curve of the reference permeability data is the solid line without data points, the flow curve of the homogenous model is the dashed line without data points. All curves of the simulated permeability data are shown as lines with data points.

The water flow curves based on the simulated permeability models from SGSIM were plotted in Figure 11. And the flow curves based on the simulated permeability models from SISIM were plotted in Figure 12. These results are discussed later in this paper.

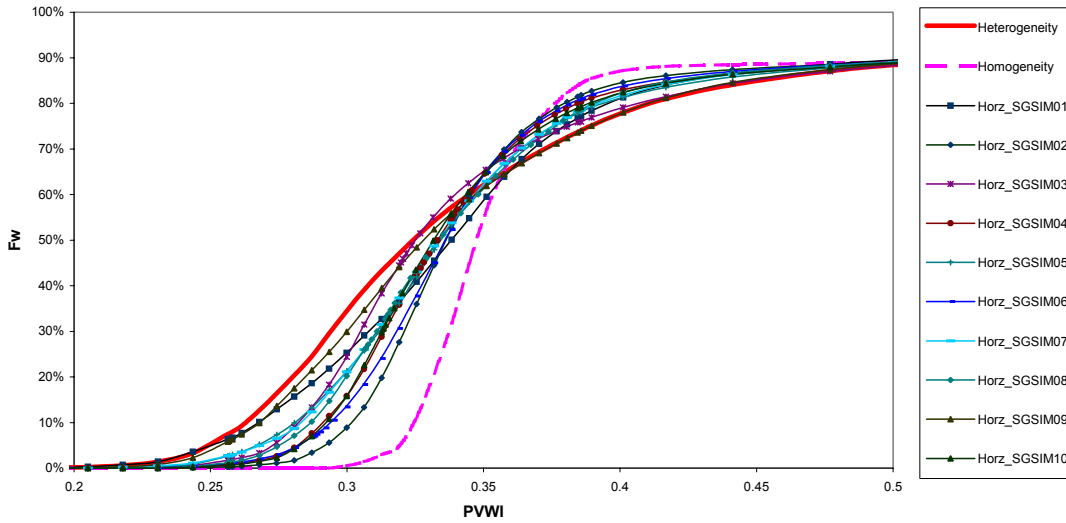


Figure 11: The water flow curves of TI data and SGSIM realizations.

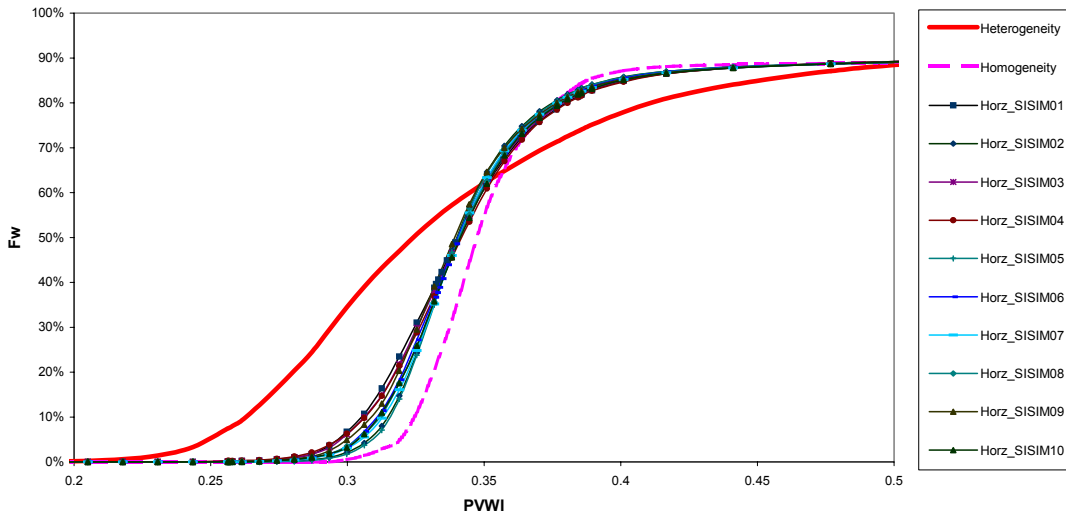


Figure 12: The water flow curves of TI data and SISIM realizations.

Small Training Image

A small 60 by 90 pixel image was extracted from the center of the training image. The image was transformed into a GSLIB format data file, which is called STI data. Figure 13 shows the small STI data. The geological shapes appear larger. A continuity is clearly shown in the horizontal direction. The STI data contains 5,400 data with a mean of 161 mD and a standard deviation of 39 mD.

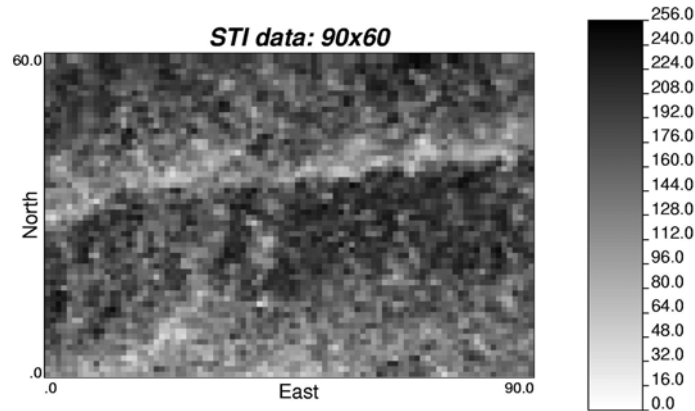


Figure 13: The small training image (STI).

The STI data were subjected to the same analysis as the full reference image data. Variograms were calculated with the Gaussian transform and the indicator transforms at 9 deciles. SGSIM and SISIM were run to predict permeability.

The 10 realizations of SGSIM are shown in Figure 14, and the 10 realizations of SISIM are shown in Figure 15. The continuity in the horizontal direction is clearly seen in every realization. The SGSIM realizations look smoother than the SISIM realizations. Some pure white spots are shown in the SISIM realizations that indicate some very low values.

The reference STI data and all realizations were changed into Eclipse data format. The grid system of 90 x 60 x 1 was used for the reservoir model. The size of the reservoir model was about one tenth of the previous one, 180 ft in length, 120 ft in width and 20 ft in depth. The rest of the settings were kept the same. Figures 16 and 17 are the water production curves from the flow simulation with the permeability data from both SGSIM and SISIM.

Heterogeneity and Uncertainty

When looking at the flow simulation results (Figures 11, 12, 16 and 17), it can be easily seen that all the estimated data lines fall between the true data and the homogenous lines. This may suggest that the sequential simulations tend to reduce the heterogeneity.

For the TI data, the SGSIM data lines are quite variable. The lines of Horz_SGSIM09 and Horz_SGSIM01 are very close to the TI data line, and some lines are far away from the TI data line. The SISIM data lines are clustered and are closer to the homogenous line. The shape of the lines is also similar to the shape of the homogenous line. The uncertainty in the SISIM data is apparently larger than that of the SGSIM data. The nugget effect had been suspected to be one of the reasons for the large uncertainty. However, after lowering the nugget effect, the uncertainty in the flow curves was still the same. To find out the reason, the Horz_SGSIM09 and the Horz_SISIM01 were chosen to show water saturation at the time of 0.25 pore volume of water

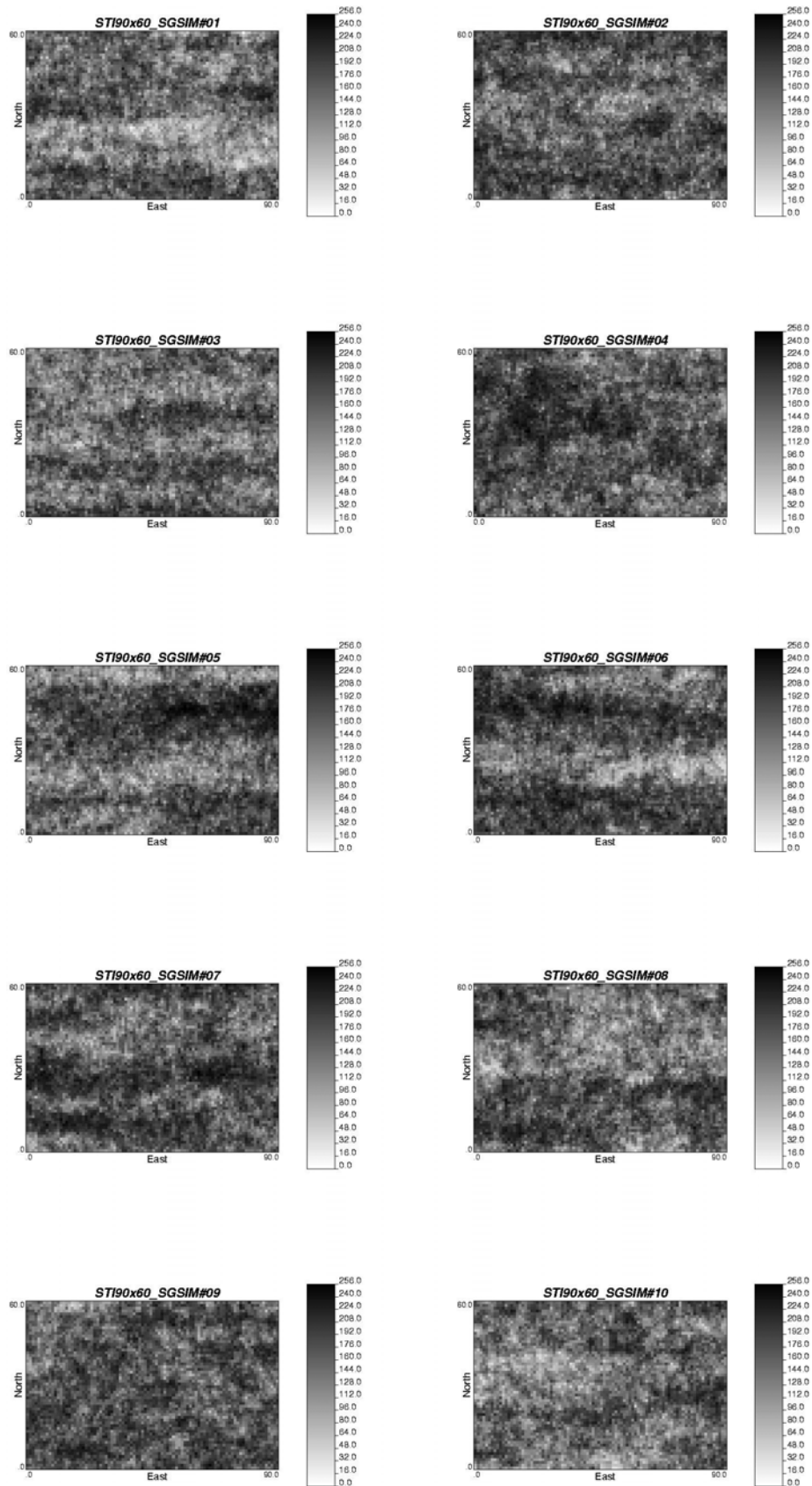


Figure 14: Ten SGSIM realizations of the STI.

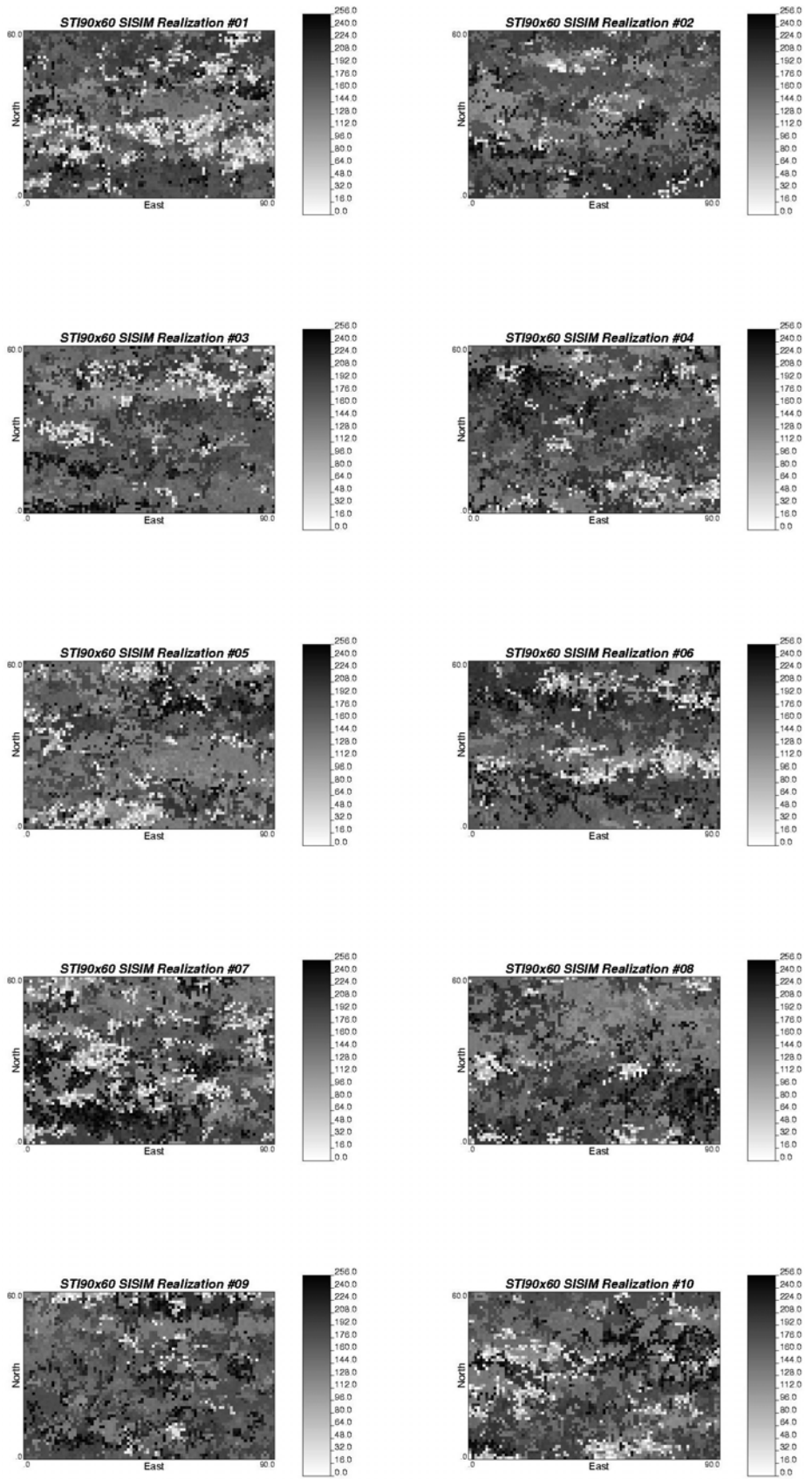


Figure 15: Ten SISIM realizations of STI.

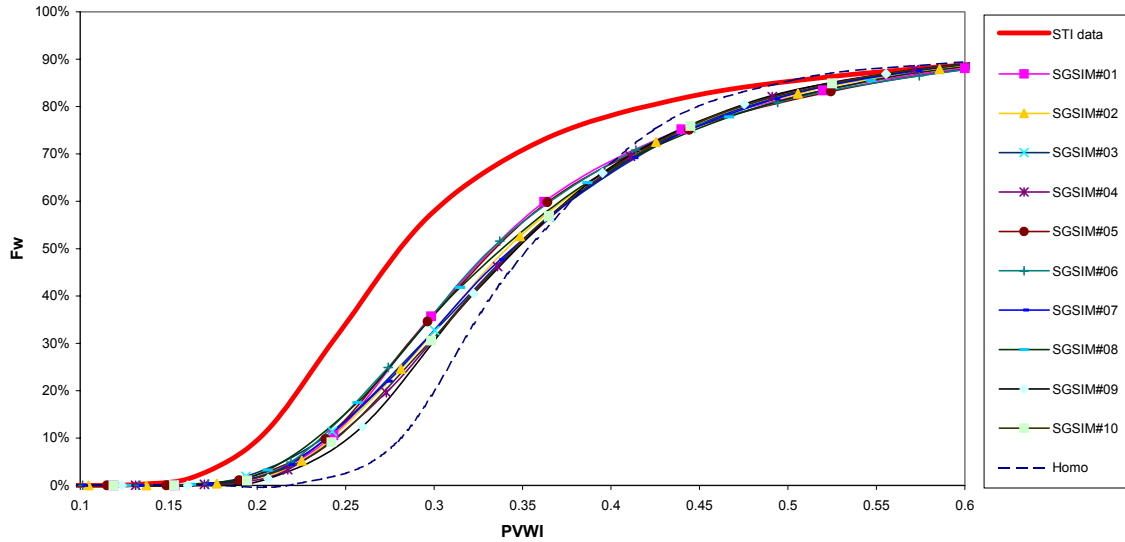


Figure 16: The flow curves of STI data and SGSIM data.

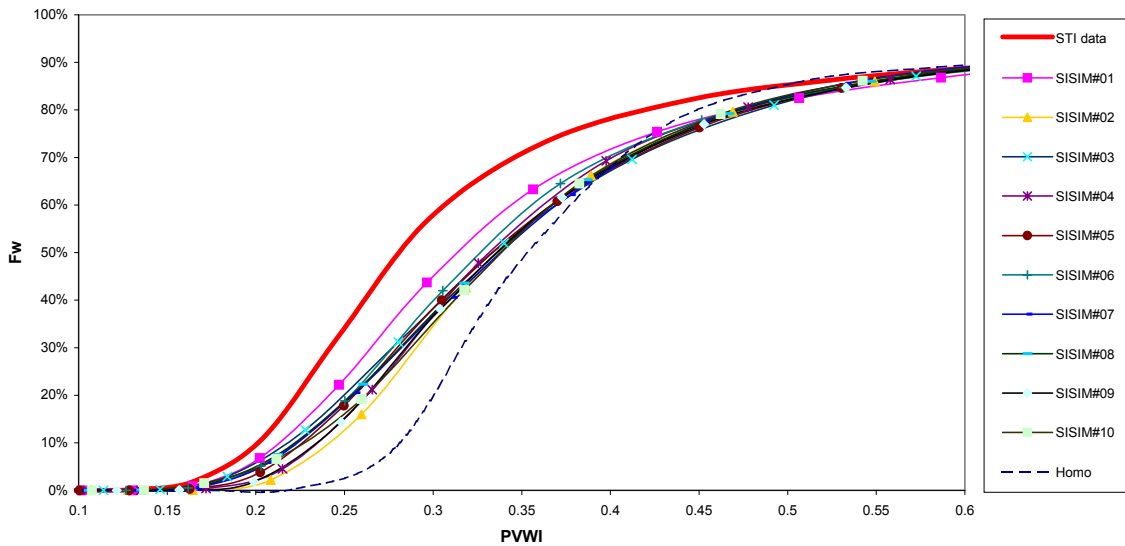


Figure 17: The flow curves of STI data and SISIM data.

injected; the 2D results are shown in Figures 18 and 19 respectively. The water breakthrough in Horz_SGSIM09 is due to water fingering. While the water front in the Horz_SISIM01 was nearly flat and did not reach the production well. The permeability in X-direction in both reservoir models is shown in Figures 20 and 21. The light color is the high permeability and the dark color is the low permeability. The high permeability zones in the Horz_SGSIM09 are mostly connected in the X-direction from the injection well to the production well. But in the Horz_SISIM01, the high and low permeabilities were evenly distributed so that the connectivity of the high permeability zones was fairly poor. The flat water front, therefore, looks like water flooding in a homogeneous formation.

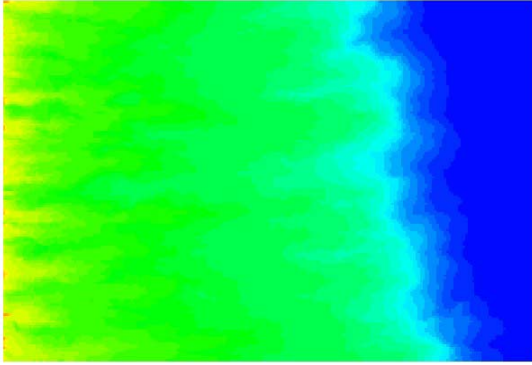


Figure 18: Horz_SISIM01, water saturation at 0.25 PVWI.

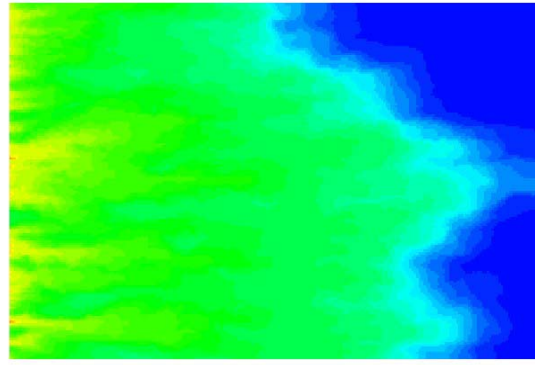


Figure 19: Horz_SGSIM09, water saturation at 0.25 PVWI, water breakthrough.

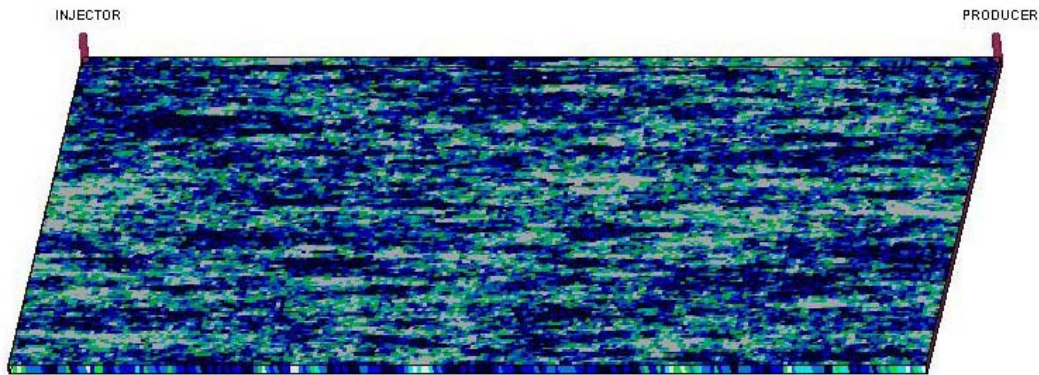


Figure 20: Horz_SGSIM09 - permeability in X-direction, the light color is high permeability and the dark color is low permeability.

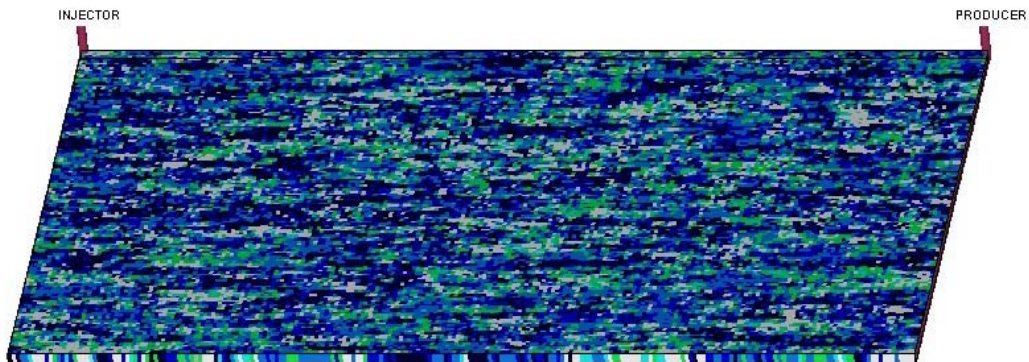


Figure 21: Horz_SISIM01 - permeability in X-direction.

From these results, it can be said that the connectivity of the high permeability zones is very important in simulating the heterogeneity in this training image. The unconditional simulation using variogram-based Gaussian and indicator techniques generally cannot maintain the connectivity. Therefore, the simulated data has less heterogeneity and the flow simulation results tend towards the homogenous line. In the indicator simulations, the high and low values are more evenly distributed so that the connectivity of high permeability zones was very poor, which resulted in poor reproduction of the reference heterogeneity.

For the small image, the simulated data lines are all clustered and away from the STI data line. The uncertainties are bigger than the uncertainty in the SGSIM data to TI data. We would expect more variability with the STI data because of the relatively smaller domain.

Comparing the two figures of flow curves of SGSIM and SISIM with STI data, the SGSIM data has a slightly larger uncertainty than the SISIM data. This is different from the simulation results based on TI data. The permeability in the X direction of SGSIM#01, SISIM#01 and the STI data are shown in Figures 22, 23 and 24. The permeability from the STI data shows that there are many very high and very low permeabilities in the reservoir. However, in the permeabilities from the simulated data, the points of very high and very low permeabilities are much less. The reduced number of low and high permeability values is due to the scaleup since the histogram of permeability values is reproduced by the simulation at a small scale. The reduction in low and high permeability values may explain why the heterogeneity in the simulated data have less of an effect than the STI data.

For the small domain, the number of high and low values became important in simulating the heterogeneity. The sequential simulations tend to have averaged values and reduced the heterogeneity effect. Therefore, a large uncertainty was created to simulate the data that had a large number of very high and low values. Indicator simulation preserves the high and low values better because of the inherent patchiness.

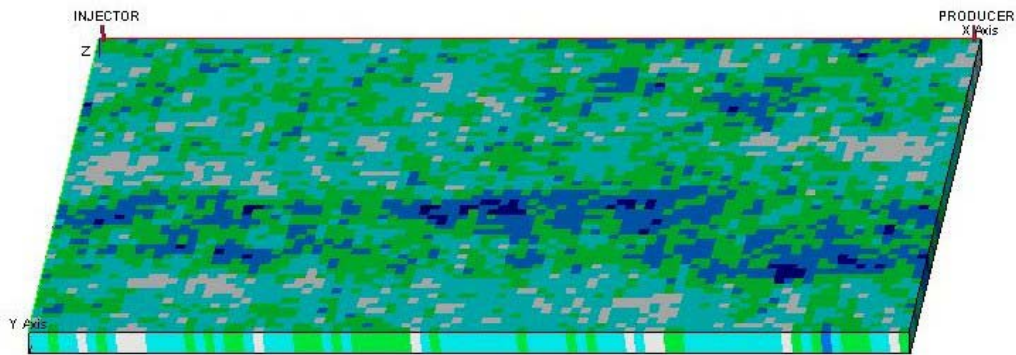


Figure 22: SGSIM#01 - permeability in X direction.

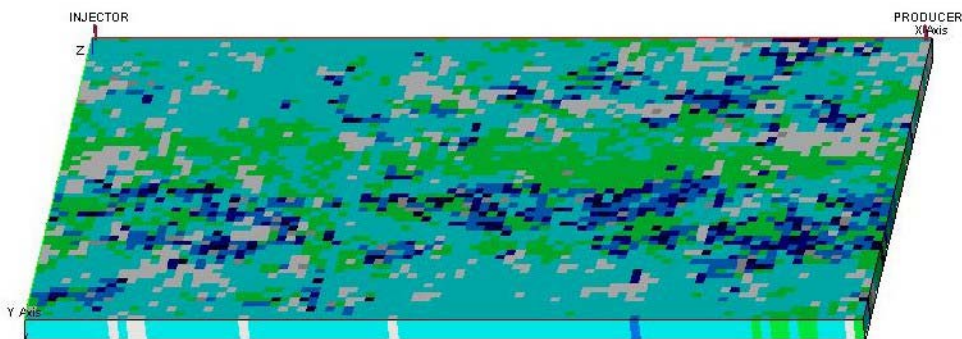


Figure 23: SISIM#01 - permeability in X direction.

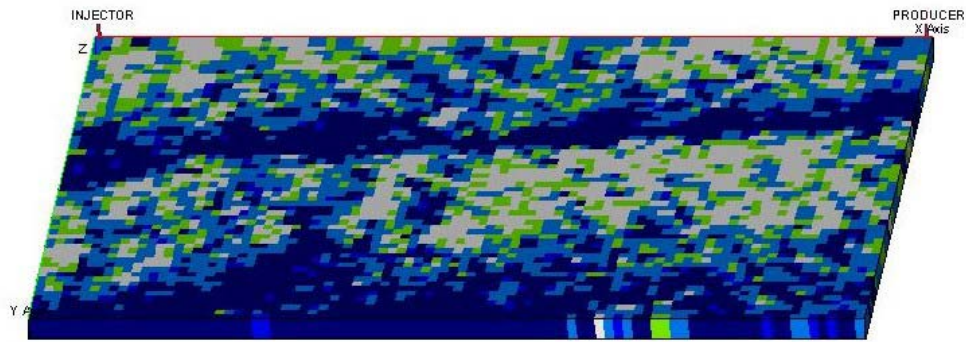


Figure 24: STI data - permeability in X

Conclusion

The implementation details of both Gaussian and indicator simulation have been shown. The distribution of permeability must have some extreme high and low values for the heterogeneity to really matter; otherwise, the well and boundary conditions dictate the flow results.

The connectivity of high and low permeability zones is an important factor in flow simulation. The conventional Gaussian and indicator sequential simulations do not preserve the connectivity of the extreme values; therefore, the flow response of the geostatistical realizations does not reproduce the effect seen with the reference image.

The indicator simulation tends to evenly distribute the high and low values leading to an overall poor model of connectivity. The flow results appear more like a homogenous reservoir than the known heterogeneous reference image.

For the small training image, the connectivity of high permeability zones is easier to inject in the model, but the number of very high and low values in the simulated data becomes very important. The sequential simulations for this sub-area tend to have too few very high and low values; the short scale structure could be reduced to improve this smoothing.

The reference image and all files related to this exercise are available to CCG members on request.

References

- *Eclipse: Reference Manual*, Schlumberger Technology Corporation, 2002
- Deutsch, C. V. and Journel, A. G., *GSLIB: Geostatistical Software Library and User's Guide*, Oxford University Press, New York, 2nd Ed., 1998a.
- Deutsch, C. V., *MIN E 612: Geostatistical Methods for Modeling Earth Sciences Data*, University of Alberta, 1998b.